UDC621.385.833:669.112.227.1:669.293

AP-FIM Analysis of Niobium Distribution at Austenite Recovery Stage in Hot-Deformed Steels

Naoki Maruyama*1 Ryuji Uemori*2
Yoshio Terada*3 Hiroshi Tamehiro*2

Abstract:

The distribution of niobium in hot-deformed HSLA steels in the early stage of austenite recovery was investigated by an atom-probe field ion microscope (AP-FIM). It was confirmed that the onset of recovery can be inhibited by solute niobium randomly dispersed in the austenite matrix. Simple calculation conducted by considering the interactions between the solute atoms and defects indicates that the strong retardation ability of niobium as compared with titanium, vanadium, and molybdenum is a result of larger impurity diffusion coefficients and solute-lattice defect interactions. The AP analysis of a 0.10Nb steel revealed that not only single solute atoms but also niobium-nitrogen pairs exist in the early stage of recovery. It is possible that the niobium-nitrogen pairs play an important role in impeding the austenite recovery of hot-deformed steels. It was also shown that the AP-FIM is a useful technique that can be used to quantitatively evaluate the distribution of the microalloying elements in steels at an atomic level.

1. Introduction

It is widely known that the small addition of niobium to a steel markedly inhibits the recovery and recrystallization of hot-deformed austenite (γ)[1-11]. The solute drag effect[1,2] of niobium segregated at grain boundaries and the grain-boundary pinning effect[3-6] of fine niobium carbonitrides have been advanced as mechanisms for retarding the recrystallization of the hot-deformed austenite, although the presence of niobium segregated at the grain boundaries is not directly confirmed yet. Presuming from past reports, it would be certain that these two mechanisms both operate to retard the recrystallization of the hot-worked austenite in actual steels.

When attention is focused on recovery as the prior stage of recrystallization, since the addition of niobium retards the start of recovery[8], it is presumable that another retardation mechanism such as pinning of dislocations and vacancies by solute atoms and strain-induced precipitates are operating[10-11]. In this case, however, strain-induced precipitate particles are predicted to measure only a few nanometers or less in size and are not easy to identify by conventional microscopic techniques such as electron microscopy. It is

*1 Advanced Technology Research Laboratories
*2 Steel Research Laboratories
*3 Kimitsu R & D Lab.

also extremely difficult to estimate the distribution of niobium quantitatively in the early stage of recovery or recrystallization from average composition determined by chemical analysis techniques. For these reasons, the distribution and role of niobium in the early stages of recovery and recrystallization are not made fully clear yet.

The atom-probe field ion microscope (AP-FIM) is one of a useful analytical techniques that can clarify the distribution of the elements at an atomic level[12,13]. It can be used for analyzing the composition, structure and distribution of ultrafine precipitates and clusters 2 to 3 nm or less in size present in metallic materials.

To clarify the role of niobium in inhibiting the recovery of a hot-deformed austenite microstructure, this study investigated the distribution of niobium in the early stage of austenite recovery by AP-FIM, and discussed the reason why niobium has a higher ability to inhibit the recovery of hot-deformed austenite than other microalloying elements such as titanium, vanadium and molybdenum.

2. Experimental Procedures

Test steels were based on a low-carbon silicon-manganese steel with a trace titanium of 0.017 mass% and varied in the niobium content in four steps from 0 to 0.122 mass%. They were melted in a 150-kg vacuum furnace and rolled to a thickness of 20 mm. **Table 1** shows the chemical compositions and manufacturing conditions of the test specimens. To simulate the initial stages of recovery and recrystallization in hot working, the test specimens were solution treated for 1.2×10^3 s at 1,250°C, rapidly cooled by helium gas to a deforming temperature of 950 to 1,150°C in about 1 s, held at the temperature for 10 s, and then compressed in two steps at a strain rate of 10 s^{-1}. **Fig. 1** shows the test conditions of the double compression test.

In this experiment, softening ratio X_s was used to evaluate the recovery and recrystallization behavior. The softening ratio was determined from $X_s = (\sigma_m - \sigma_2)/(\sigma_m - \sigma_1)$, where σ_1 and σ_2 are yield stresses in the first and second compression, respectively, and σ_m is the maximum stress in the first compression[9]. X_s was calculated by using $\varepsilon = 0.05$ as the amount of strain to provide the yield stress. The strain rate of 10 s^{-1} and strain of 0.15 correspond to the working conditions under which static recovery and recrystallization take place[9].

The hot-deformed austenite microstructure was observed by a TEM (transmission electron microscope: Hitachi HF-2000) and an AP-FIM (VG FIM-100) to clarify the distribution of niobium. The TEM was used to confirm the presence of relatively large precipitates more than around 5 nm. Thin-foil specimens for the TEM were prepared by the twin-jet electropolishing method using a mixed solution of 5% perchloric acid and 95% acetic acid. Needle-like specimens for the AP-FIM were prepared by the electropolishing method using a mixed solution of phosphoric acid and chromic acid. Ne gas was used as the imaging gas for FIM observation. The AP analysis was performed under the conditions of V_{DC} = 5-15 kV and the pulse ratio V_P/V_{DC} = 16%.

Table 1 Chemical compositions (mass%) and manufacturing conditions of test steels

Steel	C	Si	Mn	P	S	Cu	Ni	Ti	Nb	N
NB0	0.040	0.15	1.50	0.009	0.002	0.28	0.27	0.017	-	0.0021
NB5	0.040	0.15	1.47	0.009	0.002	0.28	0.27	0.017	0.047	0.0023
NB10	0.039	0.15	1.49	0.009	0.002	0.28	0.27	0.017	0.098	0.0024
NB12	0.039	0.15	1.49	0.009	0.002	0.28	0.27	0.017	0.122	0.0027

Manufacturing conditions : 150kg vacum melting→rolling (195mm→20mm, finish rolling temperature > 950°C)→water cooling

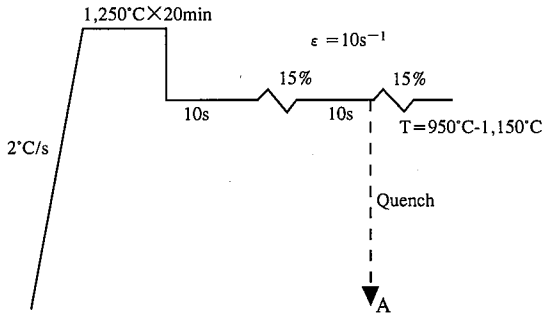

Fig. 1 Test conditions of thermal cycle simulator

3. Experimental Results

3.1 Effects of niobium content and deforming temperature on softening behavior

Fig. 2 shows the effects of the niobium content and deforming temperature on X_s. X_s = 1 means that the recovery and recrystallization of hot-worked austenite are fully completed. As is evident from **Fig. 2**, the recovery and recrystallization of hot-deformed austenite are retarded to an increasing degree with increasing niobium content. When the working temperature is 950°C, for example, partial recrystallization occurred in the specimen of no niobium addition (NB0)[9], whereas no recovery and no recrystallization in the specimen of 0.098%-niobium content (NB10) and 0.122%-niobium content (NB12). Thus, it is evident from the result that the recovery and recrystallization of hot-deformed austenite are markedly inhibited by the niobium addition.

3.2 Distribution of niobium in the early stage of recovery

This section presents the results of observation conducted to clarify the presence or absence of strain-induced precipitate. The steel NB10 with a niobium content of 0.098% solution-treated at 1,250°C, deformed by 15% at 950°C and a strain rate of 10 s^{-1},

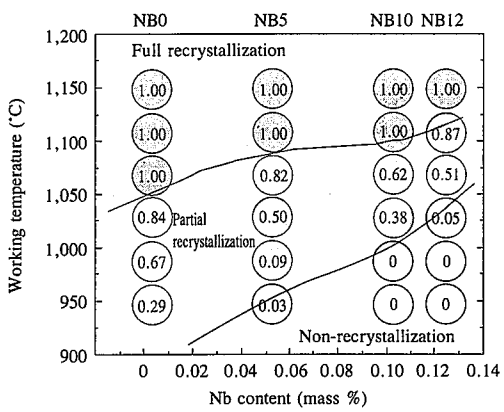

Fig. 2 Effects of working temperature and niobium content on softening ratio X_s

held at the temperature for 10 s was examined by the TEM and AP-FIM (condition A in **Fig. 1**).

3.2.1 TEM observation

Photo 1 shows the extraction replica TEM micrograph of the precipitates. Carbonitrides of titanium and niobium about 20 to 30 nm in diameter, are observed in the TEM micrograph. Since it is difficult to think that these coarse precipitates were formed during holding for 10 s after deforming, they are probably precipitates that did not go into solid solution during the solution treatment at 1,250°C. The TEM observation of thin-foil specimens of the same steel found no precipitates exceeding at least 2 nm in particle size, excluding the above-mentioned carbonitrides. Thus, these TEM observation results strongly suggest that niobium is present in the solute condition at an early stage of recovery.

3.2.2 AP-FIM observation

It is reported that niobium precipitates of a few nanometers in size can be observed by the AP-FIM in the case that it is not observable by the TEM[14]. **Photo 2** shows a typical sequence of FIM images with field evaporation of atomic planes layer by layer from the surface of specimen. It is known that when niobium carbides, a few nanometers in size, are present in the steel, they are observed as particularly bright regions as compared with the iron matrix and that the bright regions do not move by the field evaporation of a few atomic planes[13]. However, such regions were not observed in the FIM micrographs as shown in **Photo 2**. The bright spots indicated by the arrows in the micrographs disappeared each time one atomic plane is field evaporated. This denies the presence of niobium at least as clusters or precipitates. The present experimental study performed similar FIM observations on more than 500 atomic planes (equivalent to a total depth of approximately 140 nm or more) and obtained the same results.

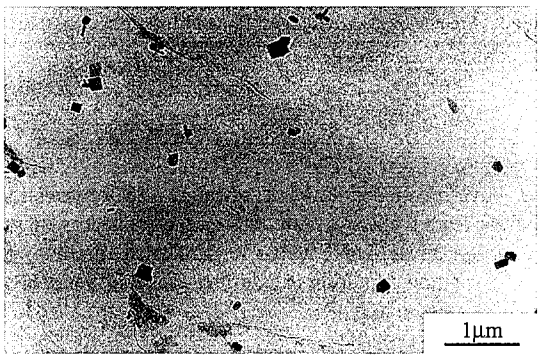

Photo 1 Extraction replica image of NB10 (Treatment A in **Fig. 1**)

Fig. 3 shows the AP spectrum of the matrix of the unrecovered steel (NB10). In this spectrum, Nb^{3+} ions, Nb^{2+} ions, and NbN^{3+} ions were detected at M/ne = 31.0, M/ne = 46.5, and M/ne = 35.5, respectively. Detected number of niobium ions was 21, and the total number of ions detected was 30,000. The total number of niobium ions detected was converted into a niobium concentration of 0.070 ± 0.015 (at%) and was almost equivalent to a niobium addition of 0.062 at%.

Fig. 4 shows a niobium concentration profile obtained from above-mentioned three types of niobium ions. The niobium concentration profile was constructed by dividing all of the detected ions into 250 blocks of 120 ions each and determining the niobium concentration in each block. Individual data points in the concentration profile indicate the average concentration of 120 ions. If precipitates are present in the steel, peaks appear in correspondence with the size of the precipitates. Since 25 ions were detected per one (100)Fe atomic plane, the number of detected ions was converted to depth by {Fe (100) plane spacing} × {(number of detected ions)/25} and plotted along the horizontal axis of the concentration profile. In **Fig. 4**, no peaks derived from precipitates were observed at all. Thus, this result indicates that niobium exists as solid solution in the matrix.

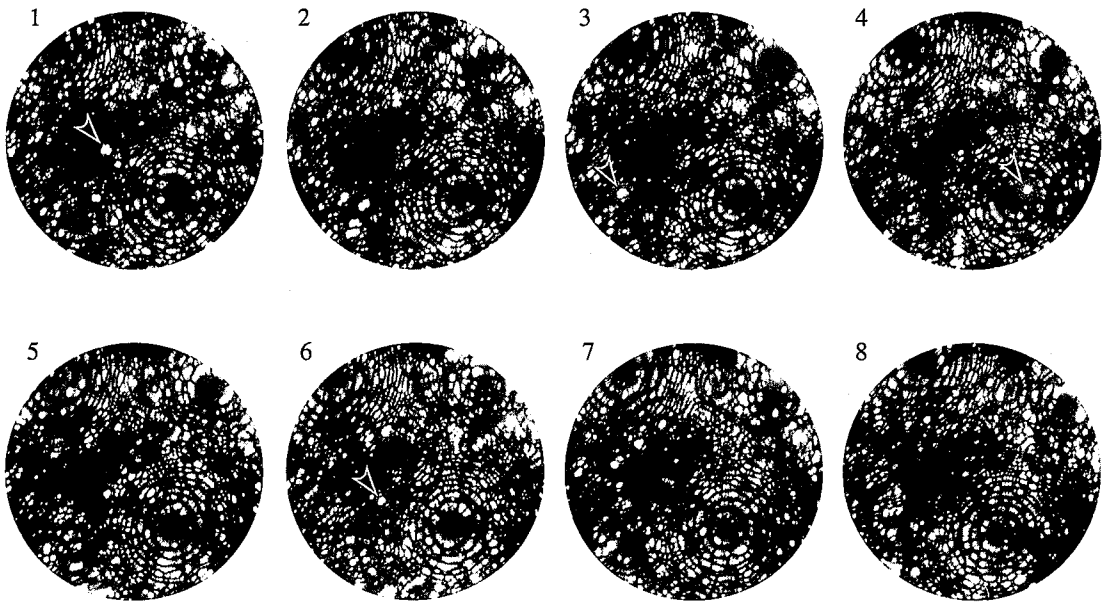

Photo 2 Typical sequence of images with layer-by-layer field evaporation (steel NB10)

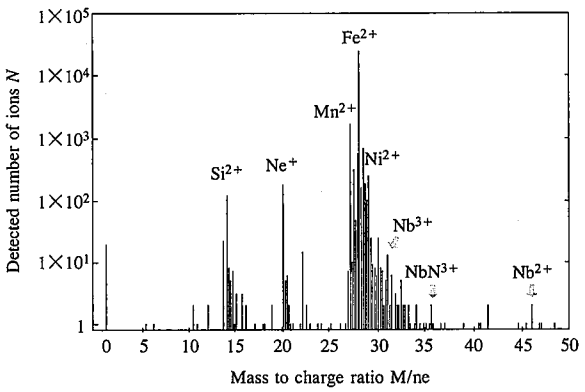

Fig. 3 AP spectrum of NB 10 (Treatment A in **Fig. 1**)

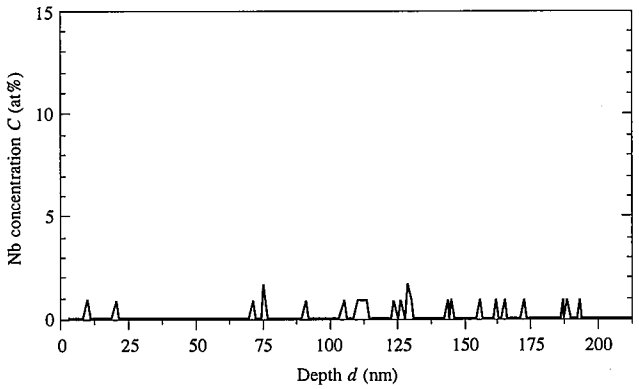

Fig. 4 Niobium concentration profile of NB 10 (Treatment A in **Fig. 1**)

Fig. 5 shows the auto-correlation function[12] of niobium obtained from the same three types of niobium ions as shown in **Fig. 4**. The auto-correlation function $R_{x\text{-}x}(k)$ statistically represents the distribution of atoms of a particular species X in the matrix, and is calculated by

$$R_{X\text{-}X}(k)=\frac{N}{N-k}\cdot\frac{\sum_{i=1}^{N-k}(X_i-\overline{X})(X_{i+k}-\overline{X})}{\sum_{i=1}^{N}(X_i-\overline{X})} \quad \cdots\cdots(1)$$

where X_i is the average concentration of the X atoms in the i-th block. One block contains 120 ions, and k is called the auto-correlation distance. In this experimental study, k = 1 corresponds to an analytical depth of about 0.9 nm when 120 ions are analyzed. Generally, when atoms form clusters or precipitates or when the concentration fluctuates at a particular period as is the case with spinodal decomposition, the auto-correlation factor $R_{x\text{-}x}(k)$ approaches 1 at a particular k position. When the atoms exist completely randomly as in the solute condition, conversely, they exhibit no particular correlation. When the $R_{Nb\text{-}Nb}(k)$ auto-correlation diagram of **Fig. 5** is examined, few correlations are recognized. From this calculation, it can be said that niobium exists randomly in the solid solution. In **Fig. 5**, a very slight correlation is observed at the position of k = 18 (about 16 nm). This result is supported by the finding that two or more niobium ions in a single block of 120 ions were detected only twice as shown in **Table 2**.

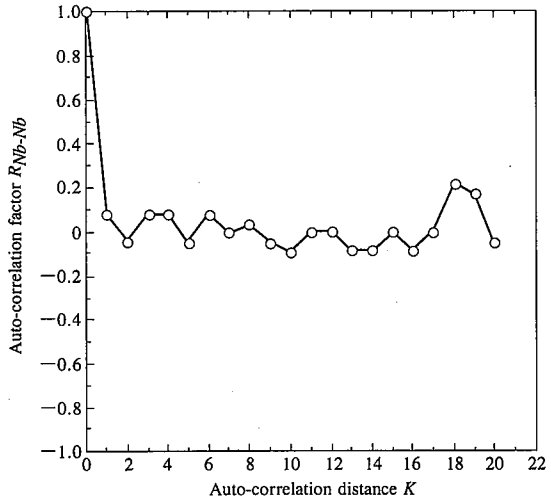

Fig. 5 Auto-correlation factor of NB 10 (Treatment A in **Fig. 1**)

Table 2 Frequency distribution of niobium ions in matrix (NB 10)

Number of Nb ions detected in one block	0	1	2	3≦
Frequency	229	19	2	0

The above-mentioned TEM observation, FIM observation, and AP analysis results clearly show that niobium clusters or precipitates are absent in the unrecovered steel. That is, niobium present in the solid solution condition is a definite cause of the delay in the beginning of recovery.

4. Discussion

4.1 Amounts of vacancies and dislocations contained in analyzed region of AP-FIM

The results of AP-FIM analysis indicated that the recovery of hot-deformed austenite is inhibited by niobium atoms in the early stages of recovery. The AP-FIM method, however, is unable to identify the positional relations between the niobium atoms and the vacancies and dislocations. Here are estimated the amounts of vacancies and dislocations considered to be observed during the AP-FIM observation.

When a metal is deformed, vacancies are formed by the cutting of dislocations. These vacancies are called excess vacancies and are distinguished from vacancies in thermal equilibrium. The amount of excess vacancies formed in a face-centered cubic (fcc) metal by working is given by[15]

$$C_v=\alpha\cdot\varepsilon^n \quad \cdots\cdots(2)$$

where ε is strain; and α and n are constants and are 10^{-2} and 2, respectively, when ε is large[14]. If Eq. (2) is applicable to the test specimens in this study, the amount of excess vacancies introduced immediately after 15% working is estimated at about 10^{-4}. This amount is considerably larger than that of the thermal equilibrium vacancies that exist at 950°C and reaches 10^{-8}. Since the diffusion of vacancies is actually extremely fast (the diffusion coefficient D of vacancies in pure iron at 950°C is around 10^{-3} cm^2/s[16]), these excess vacancies are thought to mostly disappear on dislocations during holding at 950°C for 10 s. However, the vacancy concentration in the observed specimen is not necessarily clear, because

the motion of dislocations is also inhibited by the interaction between vacancies and solute atoms as discussed in the next section.

Density of the dislocation introduced during deformation is given by the following equation[17]:

$$\rho = N \cdot \varepsilon^{\gamma} \quad \cdots\cdots(3)$$

where ε is strain; and N and γ are constants and are 10^{11} and 1, respectively[17]. From Eq. (3), the dislocation density immediately after working by 15% is estimated at around 10^{10} cm^{-2}, which can translate into a dislocation concentration of about 10^{-5} in the iron matrix.

The number of atoms seen in the FIM images of **Photo 2** is put at a few tens of thousands. Given the above-estimated vacancy and dislocation concentrations immediately after working, therefore, a few vacancies and one dislocation are considered to exist per atomic plane and every few atomic planes, respectively, in the field of view. The number of niobium atoms present in one field of view in an FIM image is at least 10 and is much larger than that of vacancies and dislocations.

In the FIM observations discussed here, at least 500 atom layers are field evaporated, and at least 100 dislocations are examined. That is, vacancies and dislocations contributing to recovery and recrystallization are thoroughly observed. By comparing the number of defects with the result that no precipitates and clusters like niobium carbonitrides, it would be certain that some interaction of solute niobium and vacancies, and dislocations are the reason for the retardation.

4.2 Effect of niobium on retardation of recovery

This section focuses on recovery as the stage in which vacancies and dislocations are rearranged, takes up niobium, titanium, vanadium and molybdenum as microalloying elements extensively added to steels, and discusses the interaction of these elements in the solute condition with lattice defects. The reason why niobium is more effective in inhibiting recovery than the other microalloying elements is discussed.

4.2.1 Effect of solute atoms on motion of vacancies

The first effect of solute niobium in retarding the beginning of recovery is the inhibition of atomic vacancy movement. According to the approximate calculation conducted by ignoring the motion of vacancy-solute atom pairs, the rate of vacancy movement in a metal containing solute atoms is apparently $\{1 + AC \cdot \exp(E^{v\text{-}s}/kT)\}^{-1}$ times the rate of vacancy movement in a pure metal[15], where C is the concentration of alloying elements; $E^{v\text{-}s}$ is binding energy of the vacancy-solute atom pair, and A is a constant. The rate of vacancy movement decreases with increasing values of C and $E^{v\text{-}s}$. Hashiguchi[18] arranged $E^{v\text{-}s}$ by the diameter difference Δd and charge difference ΔE between the solute atoms and solvent atoms. Doyama[19] has reported that in aluminum there is a negative correlation between the logarithmic solubility limit of solute elements and the binding energy $E^{v\text{-}s}$ of vacancy-solute atom pairs. When the solute atoms are put into solid solution, they undergo a greater change in internal energy due to vacancy combination as they are more likely to distort the lattice and change the surrounding electron state. Moreover, solute atoms with large values of Δd and ΔE are generally small in the solubility limit. Given these facts, their results are considered to capture the essence of binding energy. Therefore, the interaction of vacancies and solute atoms in iron about which no measured data are available is analogized in relation to the solubility limit, and the effect of niobium in inhibiting recovery is discussed in comparison with the other microalloying elements.

Table 3 gives the solubility limits of niobium, titanium, vanadium, and molybdenum in γ-iron at 1,000°C [20]. Since the solubility limit increases in the order of Nb < Ti < V < Mo, $E^{v\text{-}s}$ is considered to decrease in the order of Nb > Ti > V > Mo, based on the results of Doyama[19]. It is thus analogized that the effect of the microalloying elements in retarding the movement of vacancies also decreases in this order. Niobium is known as an element that delays the onset of recovery and recrystallization of hot-deformed austenite more greatly than titanium and vanadium[8,21]. This may be ascribed to the higher capability of niobium to inhibit the movement of vacancies and of accompanying dislocations.

4.2.2 Effect of solute atoms on movement of dislocations[22]

If the size effect and the shear modulus effect alone are considered important for the interaction between solute atoms and dislocations, the interaction force $F^{s\text{-}D}$ between screw dislocations and solute atoms varies with $|\varepsilon'_G + a \cdot \varepsilon_b|$ [23].

$$F^{s\text{-}D} \propto |\varepsilon'_G + a \cdot \varepsilon_b| \quad \cdots\cdots(4)$$

where ε'_G and ε_b are the difference of shear modulus and atomic size between solute element and iron, respectively. When the shear modulus and atomic radius of solute atoms are denoted by G_S and r_S, respectively, $\varepsilon'_G = (G_S - G_{Fe})/G_{Fe}$, and $\varepsilon_b = (r_S - r_{Fe})/r_{Fe}$. The constant a is represented by $a = 4K(1 + \nu)/(1 - 2\nu)$ in the case of screw dislocations, where ν is Poisson's ratio, and K is a bulk constant.

Table 4 shows $\| \varepsilon'_G | + a \cdot | \varepsilon_b \|$ calculated from the atomic radius and shear modulus of γ-Fe, Nb, Ti, V, and Mo. The constant a was set at a = 3 as the value that can best explain the yield behavior[23]. When the results are examined, $\| \varepsilon'_G | + a \cdot | \varepsilon_b \|$ decreases in the order of Nb > Ti > Mo > V. When attention is focused only on the relative values of the interaction force $F^{s\text{-}D}$ obtained by this simple calculation, it can be readily analogized that the interaction force between niobium atoms and dislocations is equivalent to that between titanium atoms and dislocations and is larger than that between vanadium atoms and dislocations and between molybdenum atoms and dislocations. The results of the interaction force between solute atoms and edge dislocations are the same as noted above for screw dislocations. In this way, niobium atoms are considered to present great resistance to the movement of dislocations. This may be taken as one factor responsible for the higher ability of niobium to retard recovery than the other microalloying elements.

4.2.3 Effect of diffusivity of solute atoms

It is worthwhile to consider whether or not vacancies and dislocations can be trapped by solute atoms within a very short time after deformation. The diffusion length $\sqrt{Dt}$ at 1,000°C for 1 s, calculated from the diffusion constant[24] of impurity elements in gamma iron, is 31, 27, 23, and 19 nm for niobium, titanium, molybdenum, and vanadium, respectively. On the other hand, the average distance between defects as analogized from Eqs. (2) and (3) is the order of a few tens of nanometers for both the vacancies and dislocations and is the same order of the diffusion length.

Table 3 Solubility limits of niobium, titanium, vanadium, and molybdenum in γ-iron at 1,000°C (at%)

Nb	Ti	V	Mo
0.43	0.57	0.85	1.16

Table 4 Calculated values of $\| \varepsilon'_G \| + a \cdot \| \varepsilon_b \|$ and parameters[2,4]

Solute atom in γ-Fe	Shear modulus G, (GPa)	Atomic radius r, (nm)	$\| \varepsilon'_G \|$	$\| \varepsilon_b \|$	$\| \varepsilon'_G \| + a \cdot \| \varepsilon_b \|$
Nb	37.5	0.143	0.54	0.11	0.87
Ti	45.6	0.147	0.44	0.14	0.86
V	46.7	0.132	0.43	0.02	0.50
Mo	125.6	0.136	0.54	0.05	0.70

(G_{Fe}=81.6, r_{Fe}=0.129)

Thus, these solute atoms are considered to combine with these lattice defects within a few seconds after deformation.

When specific solute atoms are compared in the diffusion length, the diffusion length is the largest for niobium and decreases for titanium, molybdenum and vanadium in that order. The order seems to agrees with the order in which the four microalloying elements are arranged by their ability to inhibit the start of recovery. Of these solute atoms, those of niobium are predicted to be the fastest to combine with the vacancies and dislocations after deformation. Coupled with the above-mentioned magnitude of the interaction force, this high diffusivity is considered as another cause of niobium's greater recovery inhibition.

4.2.4 Effect of interstitial-substitutional pairs

As already shown in **Fig. 3**, NbN^{3+} ions are detected at the position of M/ne = 35.5 on the mass spectrum. According to the results of past experiments[11,25] and calculations[26,27], the precipitation of niobium carbonitrides is reported to start at 950°C in 1 to 10 s after working. Since specimens held for 10 s after working are observed in this experiment, the Nb-N pairs are thought to be a carbonitride of the very early stage of precipitation. The reason for the formation of Nb-N pairs despite the larger amount of carbon compared to nitrogen in the material would be a difference in binding energy, because interaction parameters ε of Nb-N (ε = −115) at 1000°C is smaller than that of Nb-C (ε = −52)[28], although the ability of niobium-nitrogen or niobium-carbon pairs to capture the vacancies and dislocations as compared with niobium atoms alone is not quantitatively known yet. These substitutional-interstitial dipole pairs have been reported in the past[29-32], and a strong interaction between these dipole pairs and dislocations has been reported[29,30]. It is also reported that the hardening of a 0.15Ti steel is observed in the existence of the pairs[31]. Thus, it is possible that not only solute atoms but also these pairs play an important role on retardation of austenite recovery in hot-deformed steels. This possibility is a subject of future research.

5. Conclusions

The distribution of niobium in steels in the recovery stage of a hot-deformed austenite was observed by using an AP-FIM and a TEM. The following results were obtained:

1) The onset of austenite recovery of hot-deformed steels were retarded by the solute niobium randomly dispersed in austenite matrix.

2) Niobium in the solute condition is presumed to have a higher ability to impede the movement of vacancies and dislocations than titanium, vanadium, and molybdenum. This ability is probably responsible for the marked effect of niobium in delaying the recovery of the hot-deformed austenite. The high diffusion rate of niobium in γ-iron would be an another factor responsible for its retardation of recovery.

3) AP analysis of the steel revealed that not only single atom but also Nb-N pairs exist at the early stage of recovery. These pairs possibly play an important role in the retardation of austenite recovery in hot-deformed steels.

4) The AP-FIM method is a powerful analytical tool that can evaluate the distribution of microalloying elements in steels at an atomic level and quantitatively.

Acknowledgments

The authors wish to thank Hirofumi Morikawa of Nippon Steel Techno Research Corporation for his helpful discussions during the progress of the work.

References

1) Philips, R., Duckworth, W.E., Copley, F.E.L.: JISI. 202, 593 (1964)
2) Cahn, J.W.: Acta Metall. 10, 789 (1962)
3) Sekine, H., Maruyama, T.: Tetsu-to-Hagané. 58, 72 (1972)
4) Weiss, I., Jonas, J.J.: Met. Trans. 10A, 831 (1979)
5) Nes, E., Ryun, N., Hunderi, O.: Acta Metall. 33, 11 (1985)
6) Burke, M.G., Cuddy, L.J., Piller, J., Miller, M.K.: Mater. Sci. Tech. 4, 113 (1988)
7) Irani, J.J., Burton, D., Jones, J.D., Rothwell, A.B.: Iron Steel Inst. Spec. Rep. 104., 1967, p. 110
8) Ouchi, C., Sampei, T., Okita, T., Kozasu, I.: Hot Deformation of Austenite. J.B. Ballance edited. AIME, 1976, p. 316
9) Ouchi, C.: Tetsu-to-Hagané. 70, 291 (1984)
10) Jonas, J.J., Akben, M.G.: Met. Forum. 4, 92 (1981)
11) Yamamoto, S., Ouchi, C., Osuka, T.: Thermomechanical Processing of Microalloyed Austenite. P.J. Wray, A.J. DeArdo eds. Warrendale, PA, AIME, 1982, p. 613
12) Miller, M.K., Cerezo, A., Hertherington, M.G., Smith, G.D.W.: Atom Probe Field Ion Microscopy. Oxford, Clarendon Press, 1996
13) Uemori, R., Chijiiwa, R., Tamehiro, H., Morikawa, H.: Appl. Surf. Sci. 76/77, 25, (1994)
14) Uemori, R., Tanino, M.: J. de Physik. 48, C6-339 (1987)
15) Japan Institute of Metals: Theory of Dislocations - Its Application to Metallurgy. 1st edition. Tokyo, Maruzen, 1971
16) Koda, S.: Introduction to Physical Metallurgy. Tokyo, Corona Publishing, 1989, p. 93
17) Ham, R.K., Jaffrey, D.: Phil. Mag. 15, 247 (1967)
18) Hashiguchi, R.: J. Phys. Soc. Japan. 20, 625 (1965)
19) Doyama, M.: Phys. Rev. 148, 681 (1966)
20) Kubaschewski, O.: Iron Binary Phase Diagrams. Springer-Verlag, 1982
21) Maehara, Y., Kunitake, T., Fujino, M.: Tetsu-to-Hagané. 67, 138 (1981)
22) Maruyama, N., Uemori, R., Sugiyama, M.: Submitted to Mater. Sci. Eng. A.
23) Fleischer, R.L.: Acta Metall. 11, 203 (1963)
24) Brandes, E.A., Brook, G.B.: Smethells Metals Reference Book. 7th edition. Butterworth Heinemann, 1992, Sec. 15
25) Dutta, B., Sellars, C.M.: Mater. Sci. Technol. 3, 197 (1987)
26) Arieta, F.G., Sellars, C.M.: Low-Carbon Steels for the 90's. R. Asfahani, G. Tither eds. Warrendale, PA, TMS, 1993, p. 101
27) Liu, W.J.: Metall. Trans. 26A, 1641 (1995)
28) Zou, H., Kirkaldy, J.S.: Met. Trans. 22A, 1511 (1991)
29) Hasson, D.T., Arsenault, R.J.: Treatise on Material Science and Technology. New York, Academic Press, 1972, p. 179
30) Gouzou, J., Wegria, J., Harbraken, L.: Metall. Rep. CRM. 33, 65 (1972)
31) Pickering, H.W., Kuk, Y., Sakurai, T.: Appl. Phys. Lett. 36, 902 (1980)
32) Svensson, L.E., Henjered, A.: Mater. Sci. Tech. 1, 1094 (1985)